On the Cutoff Rates of a Multiclass OFFH-CDMA System

Elie Inaty, *Member, IEEE,*, Hossam M. H. Shalaby, *Senior Member, IEEE*, and Paul Fortier, *Senior Member, IEEE*

***Abstract*—We consider an optical code-division multiple-access (OCDMA) network that supports multiple traffic classes. Each class has different processing gain and performance requirements. In this paper, a new method is proposed to analyze the cutoff rates for a multiclass, multirate optical frequency-hopping code-division multiple-access system using fiber Bragg gratings and direct detection. This approach exploits the linear structure of passive OCDMA systems and the nominal time required to accomplish the encoding–decoding operations in such systems. A system model is presented and analyzed, based on a newly introduced bit-overlap procedure. An expression for the cutoff rate of a single-class system is derived. In addition, for a multiclass system, an expression that relates the cutoff rates of the offered classes is introduced, and it is called the service curve. It is shown that for a required quality of service guarantee, a number of active users, and a given probability of hit, the system's data rate can be increased beyond the nominal limit imposed by the physical constraint of the encoder–decoder set.**

***Index Terms*—Cutoff rate, fiber Bragg grating, multimedia network, multirate, optical frequency-hopping code-division multiple access (OFFH-CDMA), overlapping coefficient.**

I. Introduction

DUE to the emerging demand for variable and hierarchical quality of service (QoS) optical-fiber communication networks for multimedia applications where various types of data are to be transferred with different transmission speeds, future optical services will likely integrate many different streams of traffic. For this reason, integration of heterogeneous traffic with different transmission rates and QoS requirements in optical code-division multiple access (OCDMA) has received much attention lately [1]–[5].

It is important to emphasize the difference between passive OCDMA and its electrical active counterpart in order to justify our work. In fact, in active code-division multiple-access (CDMA) systems, there is a one-to-one correspondence between the transmitted symbol duration and the processing gain (PG). On the other hand, this one-to-one relation does not exist in passive OCDMA systems. For instance, decreasing the bit duration will not affect the symbol duration at the output of the optical encoder. Therefore, for a fixed PG, increasing the link transmission rate beyond a given value, known as the nominal rate, leads to bits overlap at the output of the encoder.

Optical fast frequency-hopping CDMA (OFFH-CDMA) has been proposed in [6]. In [8], we have proposed a multirate OFFH-CDMA system using fiber Bragg grating and variable PG. The idea was to respect the total round-trip time for light from a data bit to go through the encoder. Our intention was to guarantee the one-to-one correspondence between the PG and the source transmission rate. The drawback of this system is the drastic decrease in the transmitted signal power, especially for higher rate users, for which the PG becomes very low. The solution to this problem is the use of power control [5]. On the other hand, Zhang [1], [2] introduced a novel technique that lead to the generation of a new family of optical orthogonal codes (OOCs) called the *strict* OOC. Although the *strict* OOC ensures both the auto- and crosscorrelation constraints to be less than or equal to one, the cutoff rate of the system was still limited by the physical constraints of the encoder–decoder.

In this paper, the general problem we consider is by how much we can increase the transmission rates of different classes of traffic beyond the nominal permitted rates, so as to optimize performance to meet the QoS requirements. The maximum achievable class bit rate beyond the nominal rate will be noted as the cutoff rate of this class. We will show that it is possible to increase a class bit rate beyond the nominal rate without decreasing the PG of the desired user [8], or allowing any time delay between the data symbols [1].

Following the introduction, the paper is organized as follows. Section II presents the system model. In Section III, we describe a closed-form solution for the average variance of the multiple access interference (MAI) and the signal-to-interference ratio (SIR), and we quantify the effective increase in the number of hits as a function of the transmission rate. An expression for the cutoff rate for a single-class OFFH-CDMA system is derived in Section IV. In addition, a service curve is introduced and derived, which relates the cutoff rates of the offered multimedia classes in a multiclass system. Section V contains numerical results and discussions. Finally, the conclusion is presented in Section VI.

II. Multiclass System Model

Consider a multirate OFFH-CDMA communication network that supports M users in N different classes, which share the same optical medium in a star architecture [5]. The corresponding PGs for each class are given by $G_0 > G_1 > \cdots > G_{N-1}$. The encoding and decoding are achieved passively, using a sequence of fiber Bragg gratings.

Paper approved by J. A. Salehi, the Editor for Optical CDMA of the IEEE Communications Society. Manuscript received April 25, 2003; revised August 3, 2004. This paper was presented in part at the IEEE International Conference on Communications, Paris, France, June 2004.

E. Inaty is with the Department of Computer Engineering, University of Balamand, El-Koura, Lebanon (e-mail: elie.inaty@balamand.edu.lb).

H. M. H. Shalaby is with the Department of Electrical Engineering, University of Alexandria, Alexandria 21544 Egypt (e-mail: shalaby@ieee.org).

P. Fortier is with the Department of Electrical and Computer Engineering, Laval University, Quebec, QC G1K 7P4, Canada (e-mail: fortier@gel.ulaval.ca).

Digital Object Identifier 10.1109/TCOMM.2004.841999

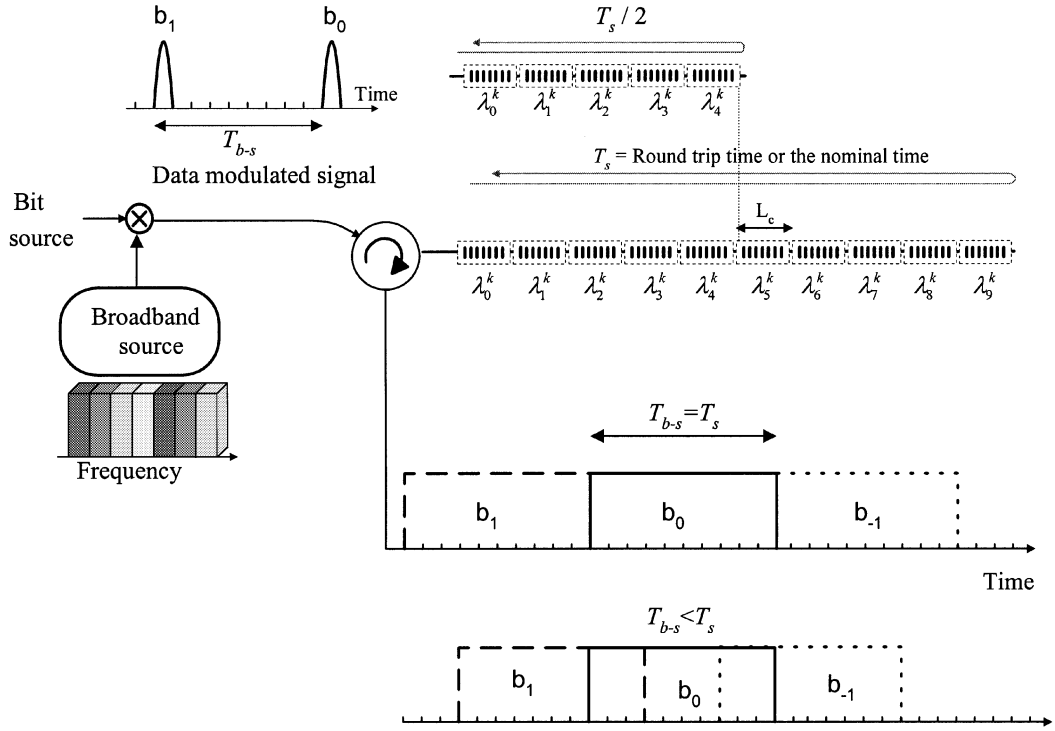

Fig. 1. OFFH-CDMA system.

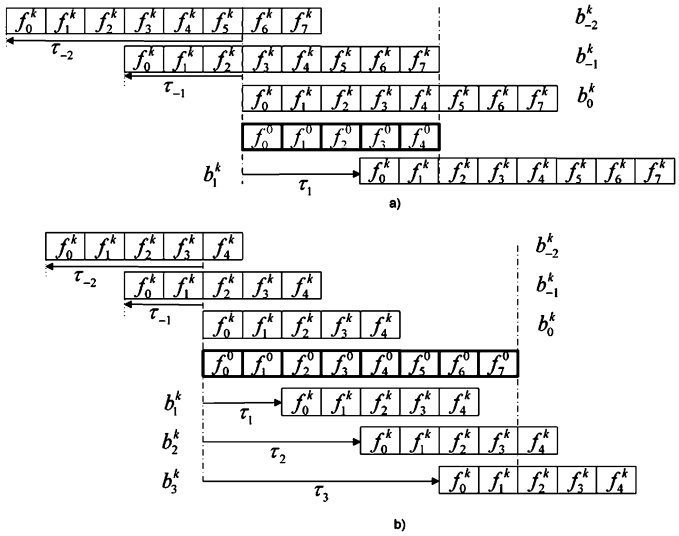

Fig. 2. Observed codes at the desired receiver from (a) the kth channel for $G_0 \leq G_k$, and (b) the kth channel for $G_0 > G_k$.

The gratings will spectrally and temporally slice an incoming broadband pulse into several components, equally spaced at chip intervals $T_c = 2n_g L_c/c$ [6], as shown in Fig. 1. L_c represents the grating length, assuming that the grating's temporal response is an ideal square wave function, c is the speed of light, and n_g is the group index. The chip duration and the number of gratings will establish the nominal bit rate of the system, i.e., the round-trip time of light, from a given transmitted bit, to be totally reflected from the encoder. This nominal bit duration in a structure of G_s gratings is given by $T_s = 2G_s n_g L_c/c$, which is normally greater than or equal to the transmission bit time period T_{b_s}. The corresponding nominal rate is $R_{n\_s} = 1/T_s$.

Due to the linearity of the gratings [first-in first-out (FIFO)], hence the linearity of the encoder–decoder set, when the data rate increases beyond R_{n_s}, multibits will be coded during the time period T_s and transmitted as revealed in Fig. 1. At a given receiver, the decoder observes practically multicode, which are delayed according to the transmission rate of the source, as shown in Fig. 2. When user k transmits using rate $R_s > R_{n\_s}$, it introduces a bit-overlap coefficient ε_s, according to which the new rate is related to the nominal rate through the following equation:

$$R_s = \frac{G_s}{G_s - \varepsilon_s} R_{n\_s}. \tag{1}$$

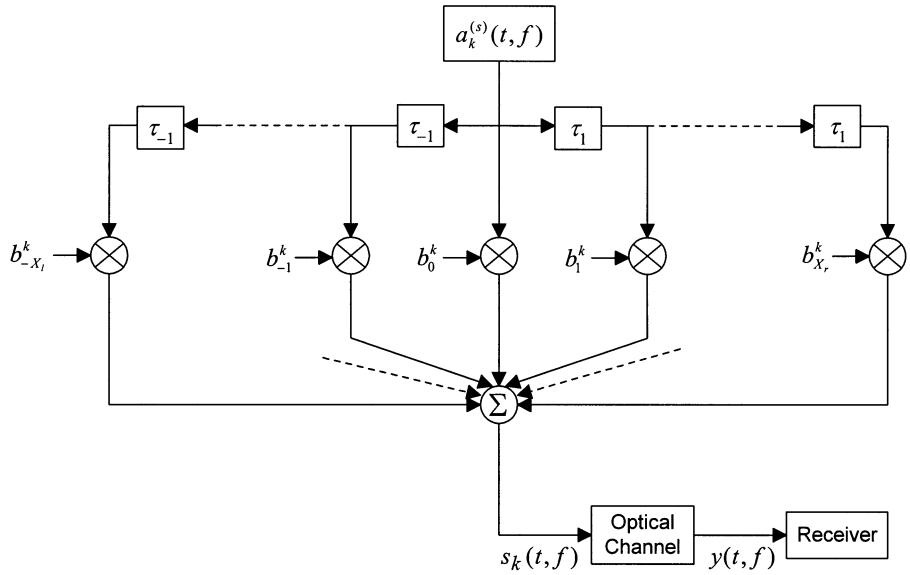

Fig. 3. Channel model.

In this paper, we assume: 1) a chip-synchronous system and a discrete rate variation; 2) all users in the *class-s*, $s \in \{0,1,\ldots,N-1\}$ have the same bit-overlap coefficient $0 \le \varepsilon_s < G_s - 1$, thus each class is characterized by $(G_s, \varepsilon_s, \beta_s)$, where β_s is the QoS requirement; and 3) a unit transmission power for all the users.

A. Signal Structure

We define $a_k^{(s)}(t,f)$ and $b_k^{(s)}(t)$ as the hopping pattern and the baseband signal, respectively, where t and f represent the time and frequency dimensions. From Fig. 2, the optical bit stream can be seen to be serial-to-parallel converted to v optical pulses. We assume that the desired user is using the *class-m*, which is characterized by a PG G_m and an overlapping coefficient ε_m. Because the bit b_X^k from the v bits is delayed by $\tau_X = X(G_s - \varepsilon_s)T_c$, this suggests that the channel model, as seen by the desired receiver, can be represented as a tapped delay line (TDL) with tap spacing of $\tau_{-1} = -(G_s - \varepsilon_s)T_c$ from the left, and $\tau_1 = (G_s - \varepsilon_s)T_c$ from the right. The tap-weight coefficients $b_X^k \in \{0,1\}$, depending on whether the transmitted bit is zero or one. The truncated TDL model, as seen by the desired receiver, is shown in Fig. 3. Accordingly, the transmitted signal is given by

$$S_k(t,f) = \sum_v b_v^k a_k^{(s)}(t - \tau_v, f). \tag{2}$$

We define v and τ_v as the index of the overlapping bit and its associated time delay, respectively. The following two lemmas will establish an expression for the total number of taps.

Lemma 1: Assume that we have an interferer k with (G_s, ε_s) and the desired user with $(G_m, \varepsilon_m) \forall\, s,m \in \{0,1,\ldots,N-1\}$. At the desired receiver end, during the nominal time period T_m, the observed total number of taps in channel k is given by

$$N_k(G_m, G_s, \varepsilon_s) = \left\lceil \frac{\varepsilon_s}{G_s - \varepsilon_s} \right\rceil + \left\lceil \frac{\Delta G + \varepsilon_s}{G_s - \varepsilon_s} \right\rceil + 1 \tag{3}$$

where $\lceil x \rceil$ is the smallest integer greater than x and $\Delta G = G_m - G_s$.

Proof: For a given rate R_s corresponding to $0 \le \varepsilon_s \le G_s - 1$ through (1), we can notice that in order for any transmitted bit b_X^k not to correlate with the desired user code during the time period T_m, the following inequalities must be satisfied.

1) *Preceding bits from the right*

$$X \ge \frac{G_m}{G_s - \varepsilon_s}. \tag{4}$$

If we use the fact that we consider discrete chip overlap, the smallest integer that satisfies (4) is

$$X = \left\lceil \frac{G_m}{G_s - \varepsilon_s} \right\rceil.$$

Thus, we can define the final bit $b_{X_r}^k$ that correlates with the desired decoder from the right as follows:

$$X_r = \left\lceil \frac{G_m}{G_s - \varepsilon_s} \right\rceil - 1 = \left\lceil \frac{G_m - G_s + \varepsilon_s}{G_s - \varepsilon_s} \right\rceil = \left\lceil \frac{\Delta G + \varepsilon_s}{G_s - \varepsilon_s} \right\rceil.$$

2) *Upcoming bits from the left*

The same analysis can be applied for the upcoming bits, but with the following inequality that must be satisfied:

$$X \ge \frac{G_s}{G_s - \varepsilon_s}. \tag{5}$$

The smallest integer that satisfies (5) is

$$X = \left\lceil \frac{G_s}{G_s - \varepsilon_s} \right\rceil.$$

Therefore, the final bit $b_{X_l}^k$ that correlates with the desired decoder from left is given by

$$X_l = \left\lceil \frac{G_s}{G_s - \varepsilon_s} \right\rceil - 1 = \left\lceil \frac{\varepsilon_s}{G_s - \varepsilon_s} \right\rceil.$$

Hence, the total number of observed transmitted codes is equal to X_r plus X_l, in addition to the normal bit b_0^k, which proves (3). ■

Lemma 2: Given an interferer k with (G_s, ε_s) and the desired user with (G_m, ε_m), the observed total number of transmitted codes from transmitter k that undergo a total overlap with the desired correlator during the nominal time period T_m, and excluding the normal bit b_0^k, is given by

$$X_t = \left\lfloor \frac{|\Delta G|}{G_s - \varepsilon_s} \right\rfloor \tag{6}$$

where $\lfloor x \rfloor$ is the highest integer smaller than x, and $|\Delta G|$ is given by

$$|\Delta G| = \begin{cases} G_m - G_s, & \text{if } G_m > G_s \\ G_s - G_m, & \text{if } G_m \le G_s. \end{cases} \tag{7}$$

Proof: The proof is divided into two parts: 1) $G_m > G_s$ and 2) $G_m \le G_s$.

1) $G_m > G_s$

In order to have a total overlap from the right, a bit b_X^k must satisfy the following inequality:

$$G_s + X(G_s - \varepsilon_s) \le G_m$$

which means

$$X \le \frac{G_m - G_s}{G_s - \varepsilon_s}.$$

The highest integer that satisfies the above inequality is

$$X_t = \left\lfloor \frac{G_m - G_s}{G_s - \varepsilon_s} \right\rfloor. \tag{8}$$

2) $G_m \le G_s$

On the other hand, b_X^k has full overlap when $G_m \le G_s$, if

$$G_s - X(G_s - \varepsilon_s) \ge G_m.$$

Therefore

$$X \le \frac{G_s - G_m}{G_s - \varepsilon_s}.$$

Thus, the final bit that has a total overlap is given by

$$X_t = \left\lfloor \frac{G_s - G_m}{G_s - \varepsilon_s} \right\rfloor. \tag{9}$$

Having (8) and (9), we can easily deduce (6), which completes the proof of the lemma. ■

The received signal at the input of the decoder is, therefore, given by

$$y(t,f) = n(t) + \sum_{k=0}^{M-1} \sum_{v=-X_l}^{X_r} b_v^k a_k^{(s)}(t - \tau_v, f)$$

where $n(t)$ is an additive white Gaussian noise (AWGN) with two-sided power spectral density $\Gamma_0/2$.

B. Decoder's Output

Without loss of generality, we assume that the correlation-matched filter is matched to the zeroth signal with class-m. The output of the noncoherent matched-filter correlator will be

$$Z_0^{(m)} = \Gamma + \int_0^{T_m} \sum_{k=0}^{M-1} S_k(t - \tau_v, f) a_0^{(m)}(t, f)\, dt$$

where Γ is a zero-mean AWGN with variance $\sigma_n^2 = N_0 T_m/4$. The MAI I_k from user k that transmits data with rate R_s can be written as

$$\begin{aligned} I_k = &\sum_{v=-X_l}^{-1} \int_0^{\tau_v} b_v^k h\left(a_k^{(s)}(t-\tau_v), a_0^{(m)}(t)\right) dt \\ &+ \sum_{v=0}^{X_t} \int_{\tau_v}^{\tau_v + T_s} b_v^k h\left(a_k^{(s)}(t-\tau_v), a_0^{(m)}(t)\right) dt \\ &+ \sum_{v=X_t+1}^{X_r} \int_{\tau_v}^{T_m} b_v^k h\left(a_k^{(s)}(t-\tau_v), a_0^{(m)}(t)\right) dt, \\ &\qquad G_m > G_s \end{aligned} \tag{10}$$

$$\begin{aligned} I_k = &\sum_{v=-X_l}^{1-X_t} \int_0^{\tau_v} b_v^k h\left(a_k^{(s)}(t-\tau_v), a_0^{(m)}(t)\right) dt \\ &+ \sum_{v=-X_t}^{0} \int_0^{T_m} b_v^k h\left(a_k^{(s)}(t-\tau_v), a_0^{(m)}(t)\right) dt \\ &+ \sum_{v=1}^{X_r} \int_{\tau_v}^{T_m} b_v^k h\left(a_k^{(s)}(t-\tau_v), a_0^{(m)}(t)\right) dt, \\ &\qquad G_m \le G_s \end{aligned} \tag{11}$$

$\forall k \neq 0$. $h(\cdot)$[1] is the Hamming function [8]. The sequences $a_k^{(s)}(t)$ and $a_0^{(m)}(t)$ are numbers representing wavelengths used at time t for the kth interferer and the desired user, respectively. Notice that $a_k^{(s)}(i) = a_k^{(s)}(i + T_s)$. In addition, we define a new performance parameter called the auto-interference, I_0, caused by the desired user's signal, and it is given by

$$\begin{aligned} I_0 = &\sum_{v=-X_r}^{-1} \int_0^{\tau_v} b_v^0 h\left(a_0^{(m)}(t-\tau_v), a_0^{(m)}(t)\right) dt \\ &+ \sum_{v=1}^{X_r} \int_{\tau_v}^{T_m} b_v^0 h\left(a_0^{(m)}(t-\tau_v), a_0^{(m)}(t)\right) dt. \end{aligned} \tag{12}$$

III. SIR Performance Evaluation

Typically, since the output interference in a large CDMA system can be approximated as Gaussian [3], it is reasonable

[1] $h(a,b) = \begin{cases} 0, & \text{if } a \neq b \\ 1, & \text{if } a = b \end{cases}$

to take the QoS requirement as meeting the SIR constraint. In this section, we derive a closed-form expression for the SIR for each class of users.

Since the user may set a connection for a particular multimedia class and modify it dynamically, the index s is a discrete random variable with a certain prior probability

$$\begin{aligned} p_k^{(i)} &= \Pr(\text{user } k \text{ chooses class} - i) \\ &= \Pr(s = i) \quad \forall\, i \in \{0, 1, \ldots, N-1\} \end{aligned} \tag{13}$$

with $\sum_{s=0}^{N-1} p_k^{(s)} = 1$, and we call $p_k^{(s)}$ the multimedia probability mass function (pmf) for user k. $I_k, \forall 0 \le k \le M-1$, is assumed to be an independent random variable. Hence, the variance of the decision variable $Z_0^{(m)}$ is

$$\operatorname{var}\left[Z_0^{(m)}\right] = \sum_{k=1}^{M-1} \sum_{s=0}^{N-1} p_k^{(s)} \sigma^2_{I_k/s} + \sigma^2_{I_0} + \sigma_n^2. \tag{14}$$

$\sigma^2_{I_k/s}$ and $\sigma^2_{I_0}$ represent the interference power caused by an active user k using class-s and the auto-interference power caused by the desired user due to overlapping, respectively, and they are given by

$$\sigma^2_{I_k/s} = E\left(I_k^2/s\right) - E^2(I_k/s) \tag{15}$$

$$\sigma^2_{I_0} = E\left(I_0^2\right) - E^2(I_0) \tag{16}$$

where $E(\cdot)$ is the expectation operator over all possible values of the overlapping bits b_X^k for $X \in \{-X_l, \ldots, X_r\}$ assuming that $\Pr(b_X^k = 1) = \Pr(b_X^k = 0) = 1/2$. Using the frequency-shifted version (FSV) system proposed in [7], $E(I_k/s)$ can be made equal to zero, and the cross terms generated from squaring the summation in $E(I_k^2/s)$ become zeros, which enables us to write (17) and (18), shown at the bottom of the page, where $H_{k,0}(\tau_i, \tau_j)$ is the continuous-time partial-period Hamming-correlation function given by

$$H_{k,0}(\tau_i, \tau_j) = \int_{\tau_i}^{\tau_j} h(a_k(t - \tau_v), a_0(t))\, dt. \tag{19}$$

If we let $q_v = \tau_v / T_c$, we can transform (19) into a discrete model as follows:

$$H_{k,0}(0, \tau_v) = T_c H_v(0, q_v) = T_c \sum_{j=0}^{q_v - 1} h(a^k_{j-q_v}, a^0_j) \tag{20}$$

$$\begin{aligned} H_{k,0}(\tau_v, T_m) &= T_c H_v(q_v, G_m) \\ &= T_c \sum_{j=q_v}^{G_m - 1} h\left(a^k_{j-q_v}, a^0_j\right) \end{aligned} \tag{21}$$

$$\begin{aligned} H_{k,0}(\tau_v, \tau_v + T_s) &= T_c H_v(q_v, q_v + G_s) \\ &= T_c \sum_{j=q_v}^{q_v + G_s - 1} h\left(a^k_{j-q_v}, a^0_j\right). \end{aligned} \tag{22}$$

Using (20)–(22), $R_k(T_m, T_s, \varepsilon_s)$ and $R_0(T_m, \varepsilon_m)$ can be written as shown in (23) and (24) at the bottom of the page.

If we define $R_k(G_m, G_s, \varepsilon_s) = R_k(T_m, T_s, \varepsilon_s)/(T_c^2/2)$, and $R_0(G_m, \varepsilon_m) = R_0(T_m, \varepsilon_m)/(T_c^2/2)$, then substitute into (15) and (16), the SIR experienced by any active user that uses class-m is

$$\text{SIR}_m = \frac{G_m^2}{\sum_{k=1}^{M-1} \sum_{s=0}^{N-1} p_k^{(s)} R_k(G_m, G_s, \varepsilon_s) + R_0(G_m, \varepsilon_m) + \sigma_n^2}. \tag{25}$$

$$E\left(I_k^2/s\right) = R_k(T_m, T_s, \varepsilon_s) = \begin{cases} \dfrac{1}{2}\left[\displaystyle\sum_{v=-X_l}^{-1} H^2_{k,0}(0, \tau_v) + \sum_{v=0}^{X_t} H^2_{k,0}(\tau_v, \tau_v + T_s) + \sum_{v=X_t+1}^{X_r} H^2_{k,0}(\tau_v, T_m)\right], & G_m > G_s \\ \dfrac{1}{2}\left[\displaystyle\sum_{v=-X_l}^{1-X_t} H^2_{k,0}(0, \tau_v) + \sum_{v=-X_t}^{0} H^2_{k,0}(0, T_m) + \sum_{v=1}^{X_r} H^2_{k,0}(\tau_v, T_m)\right], & G_m \le G_s \end{cases} \tag{17}$$

$$E\left(I_0^2\right) = R_0(T_m, \varepsilon_m) = \frac{1}{2}\left[\sum_{v=-X_r}^{-1} H^2_{0,0}(0, \tau_v) + \sum_{v=1}^{X_r} H^2_{0,0}(\tau_v, T_m)\right] \tag{18}$$

$$R_k(T_m, T_s, \varepsilon_s) = \begin{cases} \dfrac{T_c^2}{2}\left[\displaystyle\sum_{v=-X_l}^{-1} H_v^2(0, q_v) + \sum_{v=0}^{X_t} H_v^2(q_v, q_v + G_s) + \sum_{v=X_t+1}^{X_r} H_v^2(q_v, G_m)\right], & G_m > G_s \\ \dfrac{T_c^2}{2}\left[\displaystyle\sum_{v=-X_l}^{1-X_t} H_v^2(0, q_v) + \sum_{v=-X_t}^{0} H_v^2(0, G_m) + \sum_{v=1}^{X_r} H_v^2(q_v, G_m)\right], & G_m \le G_s \end{cases} \tag{23}$$

$$R_0(T_m, \varepsilon_m) = \frac{T_c^2}{2}\left[\sum_{v=-X_r}^{-1} H_v^2(0, q_v) + \sum_{v=1}^{X_r} H_v^2(q_v, G_m)\right] \tag{24}$$

A. Effective Increase in the Number of Hits

Proposition 1: For one-coincidence sequences with nonrepeating frequencies [10], the expected value of the increase in the number of hits caused by any active interferer with (G_s, ε_s) on a desired user with (G_m, ε_m) is given by

$$\begin{aligned} I_H^k(G_m, G_s, \varepsilon_s) &= \frac{1}{F}\left[\left(G_s - \frac{(G_s-\varepsilon_s)}{2}\right)X_l - \frac{(G_s-\varepsilon_s)}{2}X_l^2 \right. \\ &+ \left(G_m - \frac{(G_s-\varepsilon_s)}{2}\right)X_r - \frac{(G_s-\varepsilon_s)}{2}X_r^2 \\ &+ \left.\left(\frac{(G_s-\varepsilon_s)}{2} - |\Delta G|\right)X_t + \frac{(G_s-\varepsilon_s)}{2}X_t^2\right] \end{aligned} \quad (27)$$

and the effective increase of the number of hits due to the auto-interference is

$$I_H^0(G_m, \varepsilon_m) = 0 \quad (28)$$

where X_r, X_l, X_t, and $|\Delta G|$ are given throughout *Lemmas 1* and *2*, and F is the total number of available frequencies.

Proof: Equation (28) follows directly from the fact that for sequences with nonrepeating frequencies, we can see simply that there is no hit between a sequence and its shifted version.

- $G_m > G_s$

  Let $H_j^v, j \in \{0, 1, \ldots, G_m - 1\}$ and $v \in \{1, \ldots, X_r + X_l\}$ be the event that one of the virtual users, say, v, interferes with the desired user at chip position j. First consider virtual users from the left, thus $v \in \{1, \ldots, X_l\}$. We can easily show that the probability of hit at any chip position i, for $v \in \{1, \ldots, X_l\}$, will be

$$P(H_i^v) = \begin{cases} \frac{1}{F}, & \forall\, i \in \{0, 1, \ldots, G_s - v(G_s - \varepsilon_s) - 1\} \\ 0, & \forall\, i \in \{G_s - v(G_s - \varepsilon_s), \ldots, G_s - 1.\} \end{cases} \quad (29)$$

  Thus, the average value of the number of hits caused by a virtual user v from the left is given by

$$n_H^v = \sum_{i=0}^{G_s - v(G_s-\varepsilon_s)-1} \frac{1}{F} = \frac{G_s - v(G_s - \varepsilon_s)}{F}.$$

  On the other hand, from the right, some of the virtual interferers have full overlap with the desired user's code, and the probability of hit given in (29) can be modified as follows. For $v \in \{1, \ldots, X_t\}$, $P(H_i^v)$ can be easily shown to be

$$P(H_i^v) = \begin{cases} 0, & \forall\, i \in \{0, 1, \ldots, v(G_s - \varepsilon_s) - 1\} \\ \frac{1}{F}, & \forall\, i \in \{v(G_s - \varepsilon_s), \ldots, G_s + v(G_s - \varepsilon_s) - 1\} \\ 0, & \forall\, i \in \{G_s + v(G_s - \varepsilon_s), \ldots, G_m - 1\} \end{cases}$$

  and for $v \in \{X_t + 1, \ldots, X_r\}$

$$P(H_i^v) = \begin{cases} 0, & \forall\, i \in \{0, 1, \ldots, v(G_s - \varepsilon_s) - 1\} \\ \frac{1}{F}, & \forall\, i \in \{v(G_s - \varepsilon_s), \ldots, G_m - 1\}. \end{cases}$$

  This enables us to get the average value of the number of hits caused by virtual user v from the right as shown in the equation at the bottom of the page. Thus, the expected value of the number of hits caused by the overall overlapping process is given by

$$\begin{aligned} I_H^k(G_m, G_s, \varepsilon_s) &= \sum_{v=1}^{X_l} n_H^v + \sum_{v=1}^{X_t} n_H^v + \sum_{v=X_t+1}^{X_r} n_H^v \\ &= \frac{1}{F}\left[\left(G_s - \frac{G_s-\varepsilon_s}{2}\right)X_l - \frac{(G_s-\varepsilon_s)}{2}X_l^2 \right. \\ &+ \left(G_m - \frac{G_s-\varepsilon_s}{2}\right)X_r - \frac{(G_s-\varepsilon_s)}{2}X_r^2 \\ &+ \left.\left(G_s - G_m + \frac{G_s-\varepsilon_s}{2}\right)X_t + \frac{(G_s-\varepsilon_s)}{2}X_t^2\right]. \end{aligned} \quad (30)$$

- $G_m \le G_s$

  Following the same procedure used for $G_m > G_s$, we can prove that

$$\begin{aligned} I_H^k(G_m, G_s, \varepsilon_s) &= \sum_{v=1}^{X_r} n_H^v + \sum_{v=1}^{X_t} n_H^v + \sum_{v=X_t+1}^{X_l} n_H^v \\ &= \frac{1}{F}\left[\left(G_s - \frac{G_s-\varepsilon_s}{2}\right)X_l - \frac{(G_s-\varepsilon_s)}{2}X_l^2 \right. \\ &+ \left(G_m - \frac{G_s-\varepsilon_s}{2}\right)X_r - \frac{(G_s-\varepsilon_s)}{2}X_r^2 \\ &+ \left.\left(G_m - G_s + \frac{G_s-\varepsilon_s}{2}\right)X_t + \frac{(G_s-\varepsilon_s)}{2}X_t^2\right]. \end{aligned} \quad (31)$$

  The proposition follows by replacing $(G_s - G_m)$ in (30) and $(G_m - G_s)$ in (31) by $-|\Delta G|$. ∎

$$n_H^v = \begin{cases} \sum_{i=v(G_s-\varepsilon_s)}^{G_s - v(G_s-\varepsilon_s)-1} \frac{1}{F} = \frac{G_s}{F}, & \forall\, v \in \{1, \ldots, X_t\} \\ \sum_{i=v(G_s-\varepsilon_s)}^{G_m - 1} \frac{1}{F} = \frac{G_m - v(G_s-\varepsilon_s)}{F}, & \forall\, v \in \{X_t + 1, \ldots, X_r\} \end{cases}$$

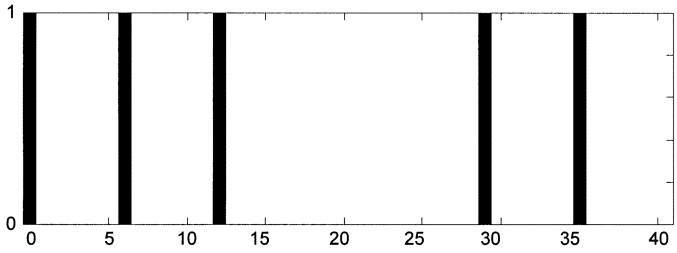

Fig. 4. Hit positions between two EHC codes for 35-chip overlap ($\varepsilon_s = 35$).

The result obtained in *Proposition 1* is very important, in the sense that one can estimate the effective increase in the number of hits as a function of the transmission rate. In Fig. 4, we plot the position of hits between two extended hyperbolic congruential (EHC) [9] codes with $G_s = G_m = 40$ and for $\varepsilon_s = 35$.

B. Average SIR

If we consider the overlapping codes generated from an active user that transmits with a rate higher than the nominal one as independent virtual active users, we can compute the average correlations given in (23) and (24), assuming one-coincidence sequences. The results are as follows:

$$\bar{H}_v^2(0,q_v) = E\left(\sum_{j=0}^{q_v-1} h^2\left(a_{j-q_v}^k, a_j^0\right) + \sum_{j=0}^{q_v-1}\sum_{\substack{i=0\\ i\neq j}}^{q_v-1} h\left(a_{i-q_v}^k, a_i^0\right) h\left(a_{j-q_v}^k, a_j^0\right)\right).$$

Due to the fact that we are assuming one-coincidence sequences, the second term in the above expression is obviously equal to zero. In addition, $h^2(a_{j-q_v}^k, a_j^0)$ is a Bernoulli random variable with values taken from the set $\{1,0\}$ with probabilities $P(H_j^v)$ and $P(\bar{H}_j^v)$, respectively. Hence

$$\bar{H}_v^2(0,q_v) = \sum_{j=0}^{q_v-1} \Pr\left(a_{j-q_v}^k = a_j^0\right) = \sum_{j=0}^{q_v-1} \frac{1}{F} = \frac{G_s - v(G_s-\varepsilon_s)}{F}. \quad (32)$$

Following the same analysis, $\bar{H}_v^2(q_v, G_m)$, $\bar{H}_v^2(q_v, q_v+G_s)$, and $\bar{H}_v^2(0, G_m)$ can be written as

$$\bar{H}_v^2(q_v,G_m) = \sum_{j=q_v}^{G_m-1} \frac{1}{F} = \frac{G_m - v(G_s-\varepsilon_s)}{F} \quad (33)$$

$$\bar{H}_v^2(q_v,q_v+G_s) = \sum_{j=q_v}^{G_s+q_v-1} \frac{1}{F} = \frac{G_s}{F} \quad (34)$$

$$\bar{H}_v^2(0,G_m) = \sum_{j=0}^{G_m-1} \frac{1}{F} = \frac{G_m}{F}. \quad (35)$$

If we substitute (32)–(35) into (23) and (24), we obtain

$$\bar{R}_k(G_m,G_s,\varepsilon_s) = \frac{1}{2F}\left[G_s + F\cdot I_H^k(G_m,G_s,\varepsilon_s)\right] \quad (36)$$

$$\bar{R}_0(G_m,\varepsilon_m) = \frac{1}{2} I_H^0(G_m,\varepsilon_m) = 0. \quad (37)$$

In addition, if we assume that the multimedia pmf is the same for every user, $p_k^{(s)} = p^{(s)}$, the average SIR for the desired user with (G_m, ε_m) will be as shown in (38) at the bottom of the page.

In (38), we have been able to separate the interference power into the normal MAI power caused by active users when $R_s = R_{n\_s}$, and the one caused by virtual users that overlap with the desired user's code when $R_s > R_{n\_s}$.

IV. Cutoff Rate

The main objective of this paper is to get a solution for the cutoff rate for each working class in the system, given $M, G_s, p^{(s)}$, and the QoS guarantee β_s for every $s \in \{0,1,\ldots,N-1\}$. The method consists of solving for ε_s using (38). Toward this end, let us begin by presenting the case of a single-class system, then generalizing the concept to a more complex scenario where we show the case of a two-class system.

A. Single-Class System

Throughout this section, we drop the subscript, which denotes the traffic class ($G_m = G_s = G$ and $\varepsilon_s = \varepsilon_m = \varepsilon$). Accordingly, it is clear that $X_t = 0$ and $X_l = X_r = \lceil(\varepsilon/G - \varepsilon)\rceil$, and the system's SIR can be written as

$$\text{SIR} = \frac{G^2}{(M-1)\frac{G}{2F} + \frac{(M-1)}{2F}\left[(G+\varepsilon)X_r - (G-\varepsilon)X_r^2\right] + \sigma_n^2}. \quad (39)$$

The problem is divided into two steps. The first step is when we consider that the required QoS allows the transmission rate to be $R_n \le R \le 2R_n$. In the second step, we assume the QoS requirements are small enough to allow $2R_n < R \le GR_n$. Thus, the critical value of ε that separates the two cases is $\varepsilon_{\text{threshold}} = G/2$, for which we can compute the threshold SIR $\beta_{\text{threshold}} = G^2/[(M-1)(G/F) + \sigma_n^2]$.

Note that F must fulfill

$$F \ge (M-1)\beta/2G \quad (40)$$

otherwise no overlap is allowed.

1) $\beta \ge \beta_{\text{threshold}}$

In this case, $0 \le \varepsilon \le G/2$; therefore $X_r = 1$. In order to respect the QoS guarantee, SIR $\ge \beta$ must be respected. Thus we can write

$$\frac{G^2}{\frac{(M-1)G}{2F} + \frac{(M-1)\varepsilon}{F} + \sigma_n^2} \ge \beta.$$

$$\text{SIR}_m = \frac{G_m^2}{\frac{(M-1)}{2F}\cdot\sum_{s=0}^{N-1}\left[p^{(s)}\cdot G_s\right] + \frac{(M-1)}{2}\cdot\sum_{s=0}^{N-1}\left[p^{(s)}\cdot I_H^k(G_m,G_s,\varepsilon_s)\right] + \sigma_n^2} \quad (38)$$

By taking the equality and solving for ε, we obtain the cutoff rate as follows:

$$\varepsilon_{\text{cutoff}} = \frac{FG^2}{(M-1)\beta} - \frac{G}{2} - \frac{F\sigma_n^2}{(M-1)} \quad \forall \beta \geq \beta_{\text{threshold}}. \quad (41)$$

2) $\beta < \beta_{\text{threshold}}$

For this situation, $G/2 < \varepsilon < G$ and the problem seems to be more complicated.

Proposition 2: For any $G/2 < \varepsilon < G$, as ε tends toward G, the SIR expression given in (39) converges to

$$\text{SIR} = \frac{G^2}{(M-1)\frac{G}{2F} + (M-1)\frac{G\varepsilon}{2(G-\varepsilon)F} + \sigma_n^2}. \quad (42)$$

Proof: See the Appendix. ■

Using the lower bound of X_r and assuming that $\sigma_n^2 = 0$, we obtain the upper bound of ε as follows:

$$\frac{G^2}{(M-1)\frac{G}{2F} + (M-1)\frac{G\varepsilon}{2(G-\varepsilon)F}} \geq \beta.$$

Therefore, the upper bound of ε is

$$\varepsilon_{\text{upper}} = \frac{2FG - (M-1)\beta}{2F}. \quad (43)$$

On the other hand, the lower bound of the cutoff rate can be derived using X_{r_extreme} (Appendix). Hence, we can write

$$\frac{G^2}{(M-1)\frac{G}{2F} + (M-1)\frac{(G+\varepsilon)^2}{8(G-\varepsilon)F}} \geq \beta.$$

$\varepsilon_{\text{lower}}$ is obtained by solving the following second-order equation in ε:

$$(M-1)\beta\varepsilon^2 + (8FG^2 - 2(M-1)G\beta)\varepsilon + (2(M-1)G^2\beta - 8FG^3) = 0. \quad (44)$$

Note that the condition in (40) insures the existence of a valid solution for (44), which is given by

$$\varepsilon_{\text{lower}} = \frac{-4FG^2 + 2G\sqrt{4F^2G^2 - (M-1)^2\beta^2}}{(M-1)\beta} + G. \quad (45)$$

Thus, the cutoff rate of the system is given by

$$\varepsilon_{\text{lower}} \leq \varepsilon_{\text{cutoff}} \leq \varepsilon_{\text{upper}} \quad \forall\, \beta < \beta_{\text{threshold}}. \quad (46)$$

It is important to note that (46) represents the bottleneck of the transmission rate for a single-class OFFH-CDMA system. Asymptotically, as F increases, it is easily seen that $\lim_{F\to\infty} \varepsilon_{\text{cutoff}} = G$. Hence, the system allows full overlap.

B. Two-Class System

In a multiclass system, instead of solving one equation for one variable ε, we expect to solve N equations for N unknowns $\{\varepsilon_0, \varepsilon_1, \ldots, \varepsilon_{N-1}\}$. For the clarity of the method and for mathematical convenience, we will present the case of a two-class system. Before continuing, let us define the following functions:

$$f(X_l) = \frac{1}{F}\left[\left(G_s - \frac{(G_s-\varepsilon_s)}{2}\right)X_l - \frac{(G_s-\varepsilon_s)}{2}X_l^2\right]$$
$$g(X_r) = \frac{1}{F}\left[\left(G_m - \frac{(G_s-\varepsilon_s)}{2}\right)X_r - \frac{(G_s-\varepsilon_s)}{2}X_r^2\right]$$
$$H(X_t) = \frac{1}{F}\left[\left(\frac{(G_s-\varepsilon_s)}{2} - |\Delta G|\right)X_t + \frac{(G_s-\varepsilon_s)}{2}X_t^2\right]$$

with $I_H^k(G_m, G_s, \varepsilon_s) = f(X_l) + g(X_r) + H(X_t)$.

Proposition 3: The functions $f(X_l)$, $g(X_r)$, and $H(X_t)$ are bounded as

$$\frac{G_s\varepsilon_s}{2F(G_s-\varepsilon_s)} \leq f(X_l) \leq \frac{(G_s+\varepsilon_s)^2}{8F(G_s-\varepsilon_s)} \quad (47)$$
$$\frac{G_m(\Delta G+\varepsilon_s)}{2F(G_s-\varepsilon_s)} \leq g(X_r) \leq \frac{(G_m+\Delta G+\varepsilon_s)^2}{8F(G_s-\varepsilon_s)} \quad (48)$$
$$-\frac{(G_s-\varepsilon_s-2|\Delta G|)^2}{8F(G_s-\varepsilon_s)} \leq H(X_t) \leq \frac{|\Delta G|(G_s-\varepsilon_s-|\Delta G|)}{2F(G_s-\varepsilon_s)}. \quad (49)$$

Proof: Omitted due to the lack of permitted space.

We will continue the analysis using only bounds of $I_H^k\ \forall\, 0 \leq \varepsilon_s < G$. To be on the safe side, the upper bound of I_H^k is adopted, and it is given by

$$I_{H\_\max}^k(G_m, G_s, \varepsilon_s) = f(X_{l\_\text{extreme}}) + g(X_{r\_\text{extreme}}) + H(X_{t\_\max}) = \frac{\left[\varepsilon_s^2 + 2(G_m - |\Delta G|)\varepsilon_s + G_s(2G_m - G_s + 2|\Delta G|)\right]}{4F(G_s-\varepsilon_s)}. \quad (50)$$

Consider a two-class system, namely, *class*-0 and *class*-1, which are characterized by $(G_0, \varepsilon_0, \beta_0)$ and $(G_1, \varepsilon_1, \beta_1)$ with $G_0 > G_1$. Using (38), the minimum SIR for each classes are given by the equation shown at the bottom of the page.

Using (50), we can easily show that

$$I_{H\_\max}^k(G_0, G_0, \varepsilon_0) = \frac{\varepsilon_0^2 + 4G_0\varepsilon_0}{4F(G_0-\varepsilon_0)}$$
$$I_{H\_\max}^k(G_0, G_1, \varepsilon_1) = \frac{\varepsilon_1^2 + 4G_1\varepsilon_1 + 4G_1(G_0-G_1)}{4F(G_1-\varepsilon_1)}$$
$$I_{H\_\max}^k(G_1, G_1, \varepsilon_1) = \frac{\varepsilon_1^2 + 4G_1\varepsilon_1}{4F(G_1-\varepsilon_1)}$$
$$I_{H\_\max}^k(G_1, G_0, \varepsilon_0) = \frac{\varepsilon_0^2 + 4G_1\varepsilon_0}{4F(G_0-\varepsilon_0)}.$$

$$\text{SIR}_0 = \frac{G_0^2}{\frac{(M-1)}{2F}\left[p^{(0)}G_0 + p^{(1)}G_1\right] + \frac{(M-1)}{2}\left[p^{(0)}I_{H\_\max}^k(G_0, G_0, \varepsilon_0) + p^{(1)}I_{H\_\max}^k(G_0, G_1, \varepsilon_1)\right] + \sigma_n^2}$$
$$\text{SIR}_1 = \frac{G_1^2}{\frac{(M-1)}{2F}\left[p^{(0)}G_0 + p^{(1)}G_1\right] + \frac{(M-1)}{2}\left[p^{(0)}I_{H\_\max}^k(G_1, G_0, \varepsilon_0) + p^{(1)}I_{H\_\max}^k(G_1, G_1, \varepsilon_1)\right] + \sigma_n^2}$$

By means of the above results, and taking $\text{SIR}_0 \geq \beta_0$ and $\text{SIR}_1 \geq \beta_1$, we obtain a system of two inequalities in the two unknowns ε_0 and ε_1 of the form

$$A_0\varepsilon_1^2 + B_0\varepsilon_0^2 + C_0\varepsilon_1^2\varepsilon_0 + D_0\varepsilon_0^2\varepsilon_1 + E_0\varepsilon_0\varepsilon_1 + F_0\varepsilon_1 + g_0\varepsilon_0 \leq H_0 \quad (51)$$

$$A_1\varepsilon_1^2 + B_1\varepsilon_0^2 + C_1\varepsilon_1^2\varepsilon_0 + D_1\varepsilon_0^2\varepsilon_1 + E_1\varepsilon_0\varepsilon_1 + F_1\varepsilon_1 + g_1\varepsilon_0 \leq H_1 \quad (52)$$

where $A_s, B_s, C_s, D_s, E_s, F_s, g_s,$ and $H_s \ \forall \ s \in \{0, 1\}$ are constants, which are function of the system parameters $G_0, G_1, \beta_0, \beta_1, K_0, K_1,$ and F.

Equations (51) and (52) draw the overlapping region of the system, meaning the region under which we can increase ε_0 and ε_1 without violating the QoS requirements. The boundary curve is obtained by taking the equalities in the above equations.

In order to get more insight to the problem under consideration, we can considerably simplify the above equation, without loss of generality, by assuming that all the classes have the same PG ($G_s = G$). In this case, $X_l = X_r = X = \lceil(\varepsilon_s)/(G - \varepsilon_s)\rceil$. Therefore, (31) is simplified to

$$I_H^k(G, \varepsilon_s) = \frac{1}{F}[(G + \varepsilon_s)X - (G - \varepsilon_s)X^2]. \quad (53)$$

Knowing that X is bounded by $(\varepsilon_s)/(G - \varepsilon_s) \leq X \leq (G)/(G - \varepsilon_s)$, the value of $I_H^k(G - \varepsilon_s)$ is simplified to

$$I_H^k(G, \varepsilon_s) = \frac{G}{F}\left(\frac{\varepsilon_s}{G - \varepsilon_s}\right). \quad (54)$$

Using (54) in (38), we obtain

$$\text{SIR}_\text{m} = \frac{G^2}{\frac{G^2(M-1)}{2F} \cdot \sum_{s=0}^{N-1}\left[\frac{p^{(s)}}{G-\varepsilon_s}\right] + \sigma_n^2}. \quad (55)$$

Again, consider a two-class system, which is characterized by (ε_0, β_0) and (ε_1, β_1). By means of the above results, and neglecting the effect of σ_n^2, (51) and (52) are simplified to

$$\left(G - p^{(1)}\right)\varepsilon_0 + \left(G - p^{(0)}\right)\varepsilon_1 - \varepsilon_0\varepsilon_1 \leq \frac{2FG^2}{(M-1)} - G \cdot \max\{\beta_0, \beta_1\}. \quad (56)$$

Equation (56) draws the overlapping region of the system, meaning the region under which we can increase ε_0 and ε_1 without violating the QoS requirements. This line is called the service curve of the system.

It is important to note that asymptotically, as F increases, (51) and (52) are simplified to

$$G_0\varepsilon_1 + G_1\varepsilon_0 - \varepsilon_0\varepsilon_1 \leq G_0G_1. \quad (57)$$

Therefore, the region has become a rectangle bounded by $\varepsilon_0 = G_0$ and $\varepsilon_1 = G_1$. Hence, the system allows full overlap for both classes.

V. Numerical Results

In comparison with previous works [1]–[8], an important contribution of this paper lies in exploiting the linear structure and the physical constraints of passive OCDMA.

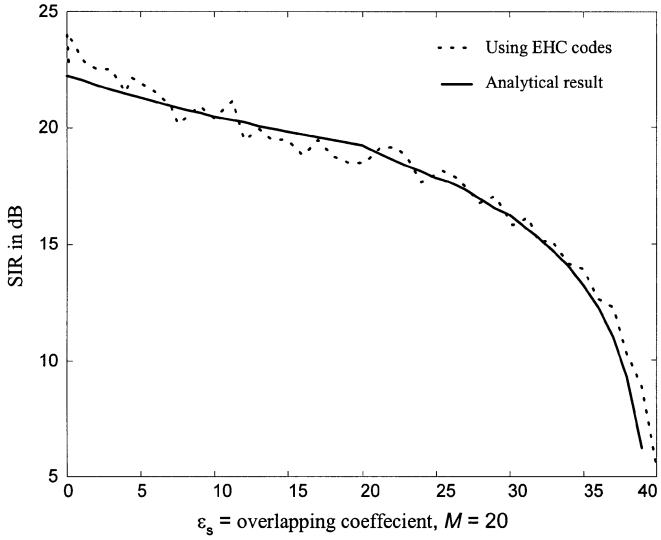

Fig. 5. System's SIR (in decibels) versus the overlapping coefficient using real codes and the analytical results.

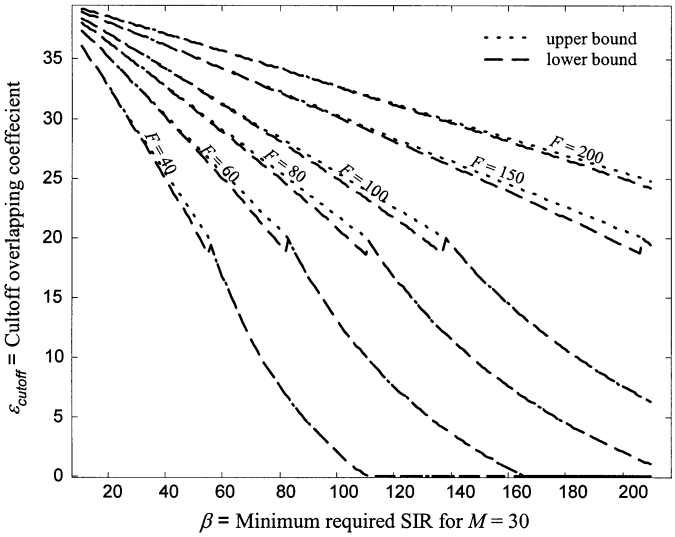

Fig. 6. Cutoff-overlapping coefficient versus the QoS requirements, and for different values of the number of available frequencies F.

First, we begin by the single-class system. In Fig. 5, we plot the SIR for an active user while varying its transmission rate, or equivalently, its overlapping coefficient using real codes in (6) and the one obtained in (40). In the numerical results that use real codes through (39), we use the EHC family of codes [9], and the sequences are generated using $F = 41$ available frequencies with $G = 40$. Notice that for $M = 20$ users and small value of the overlapping coefficient, the exact SIR exhibits some fluctuations, which make it deviate from the approximated SIR. A general observation is the drastic decrease in the system's SIR when $\varepsilon > G/2$.

The importance of the QoS requirement in determining $\varepsilon_{\text{cutoff}}$ of the system can be seen from Fig. 6. Observe that for $\beta > 100$, and assuming $F = 40$ and $M = 30$, the system does not allow any increase in the transmission rate beyond R_n. On the other hand, when $\beta < 60$, the system may allow more than $2R_n$. Notice also the importance of F in determining $\varepsilon_{\text{cutoff}}$.

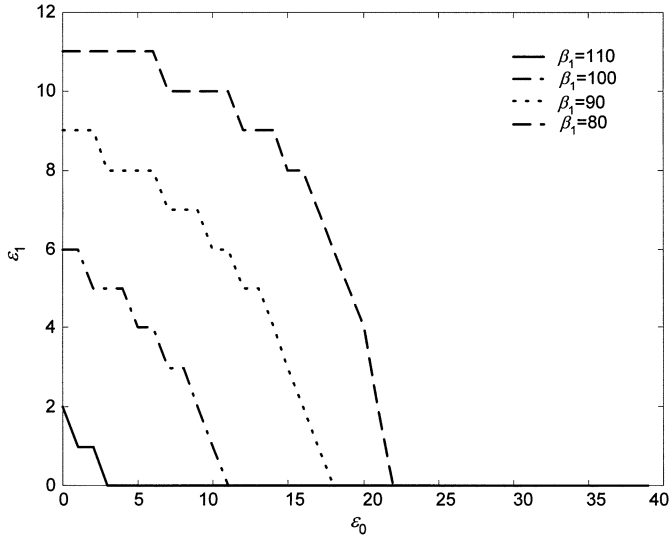

Fig. 7. Class-1 overlapping coefficient ε_1 versus the Class-0 overlapping coefficient ε_0 when we vary the Class-1 QoS β_1 and fix the Class-0 QoS $\beta_0 = 210$, the number of available frequencies $F = 80$, the total number of users $M = 20$, and the multimedia pdf $P^{(0)} = P^{(1)} = 0.5$.

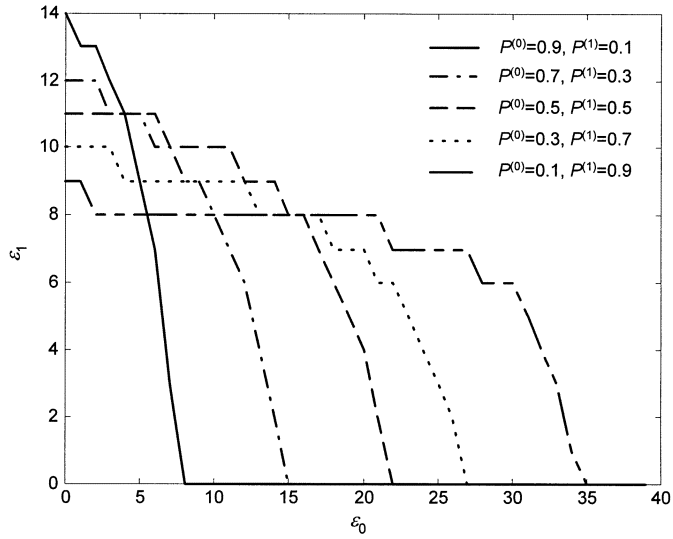

Fig. 8. Class-1 overlapping coefficient ε_1 versus the Class-0 overlapping coefficient ε_0 when we vary the multimedia pdf and fix the number of available frequencies $F = 80$, the Class-0 QoS $\beta_0 = 210$, the Class-1 QoS $\beta_1 = 90$, and the total number of users $M = 20$.

$\varepsilon_{\text{cutoff}}$ increases asymptotically as F becomes large, which is in total agreement with the analytical results discussed in Section IV.

Now we are ready to discuss the two-class case, with $G_0 = 40$ and $G_1 = 20$. Our focus is on the service curve and its dependence on the system parameters. Fig. 7 shows ε_1 versus ε_0, which corresponds to the service curve, when we vary β_1 and fix $\beta_0 = 210, F = 80, M = 20$, and $P^{(0)} = P^{(1)} = 0.5$. It is clear that when $\beta_1 > 110$, the system does not allow overlap in either class. As β_1 decreases, the overlapping region becomes wider, and the system allows more overlap for the two classes. The case $\beta_1 = 80$ represents the limiting condition, in the sense that further decreasing β_1 will not increase the overlapping region, due to the fact that only the condition on β_0 will affect this region.

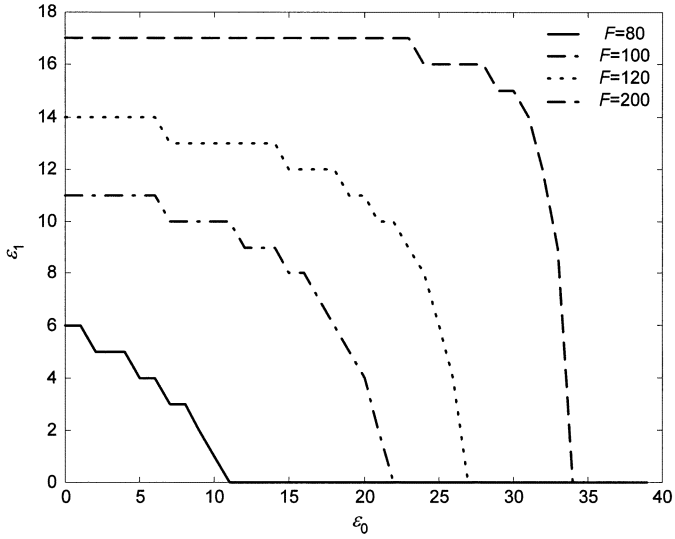

Fig. 9. Class-1 overlapping coefficient ε_1 versus the Class-0 overlapping coefficient ε_0 when we vary the number of frequencies F and fix the Class-0 and Class-1 QoS to $\beta_0 = 210$ and $\beta_1 = 100$, the number of users $M = 20$, and the multimedia pdf $P^{(0)} = P^{(1)} = 0.5$.

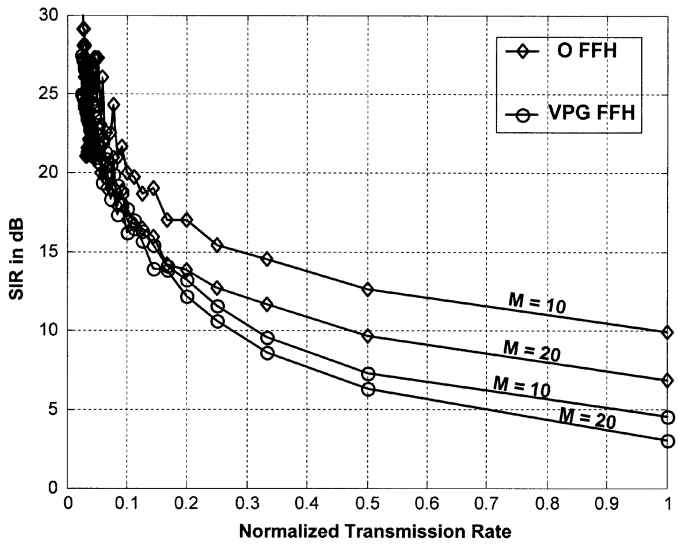

Fig. 10. SIR versus the normalized transmission rate.

On the other hand, Fig. 8 plots the service curve when varying the multimedia pdf $P^{(s)}$ while fixing $F = 80, \beta_0 = 210, \beta_1 = 90$, and $M = 20$. The important thing to notice in this figure is that when $P^{(0)} > P^{(1)}$, the system allows more relative overlap for *class*-1. As $P^{(0)} < P^{(1)}$, more relative overlap is allowed for *class*-0. In Fig. 9, the effect of F is emphasized. As it was shown in (57), as F becomes very large, the overlapping region tends asymptotically to a rectangle bounded by G_1 and G_0. Therefore, full overlap is allowed for the two classes.

Fig. 10 shows a comparison between the SIR of the newly proposed overlapped OFFH-CDMA (O-OFFH-CDMA) and the previously proposed variable PG OFFH-CDMA (VPG-OFFH-CDMA) [5] systems while varying the transmission rate. The transmission rate is normalized in the sense that it begins by zero when $\varepsilon_s = 0$ for the O-OFFH-CDMA system, and when $G_s = 40$ for the VPG-OFFH-CDMA system. The normalized transmission rate increases by increasing ε_s or decreasing G_s

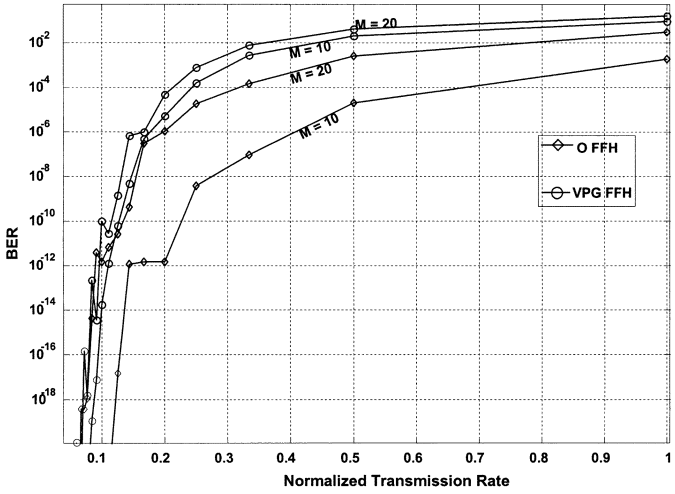

Fig. 11. Bit-error rate versus the normalized transmission rate.

for the O-OFFH-CDMA and the VPG-OFFH-CDMA, respectively. Notice that, either for $M = 10$ users or $M = 20$, the SIR for the O-OFFH-CDMA system is always greater than that of the VPG-OFFH-CDMA system.

On the other hand, Fig. 11 shows the simulated probability of error corresponding to the values of the SIR presented in Fig. 10. The simulation shows that the O-OFFH-CDMA system always outperforms the VPG-OFFH-CDMA system for different number of active users.

VI. Conclusion

The main idea from our derivations is to find and analyze the cutoff rates for a multiclass OFFH-CDMA system. A system model was presented, and the SIR was derived based on a newly proposed bit-overlap procedure. In addition, we have been able to obtain a closed-form solution for the cutoff rate of a single-class system, and a service curve for a multiclass system. Simulation and analytical results showed that it is possible to increase the transmission rate well beyond the nominal rate imposed by the physical dimensions of the encoder/decoder pairs. The importance of this paper relies on the fact that this is the first time someone considers the possibility of pushing the transmission rate beyond the nominal rate of the encoder–decoder. The idea is fundamental to most of the passive OCDMA systems. Therefore, we believe that this is an important contribution in the field of OCDMA.

On the other hand, this paper also showed a performance comparison between the multirate O-OFFH-CDMA and VPG-OFFH-CDMA. Simulations showed that our newly proposed system, the O-OFFH-CDMA system, always outperforms the VPG-O-FFH-CDMA system. In conclusion, this new system is highly recommended for multirate-multimedia applications.

It is important to note that this technique can be used for other passive OCDMA systems in order to analyze their cutoff rate. One future direction is to extend our analysis to other passive OCDMA systems, which will enable us to provide a reasonable performance comparison between these systems.

Appendix A

Proof of Proposition 2: If $G/2 < \varepsilon \leq G-1$, the integer value X_r is lower bounded by $X_{r\_\min} = (\varepsilon/G-\varepsilon)$ and upper bounded by $X_{r\_\max} = (G/G-\varepsilon)$. Using simple algebra, it can be easily shown that

$$I_H^k(X_r = X_{r\_\max}) = I_H^k(X_r = X_{r\_\min}) = \frac{G\varepsilon}{(G-\varepsilon)F}.$$

Knowing that I_H^k is a second-order equation in X_r, the maximum of I_H^k occurs at the extreme $X_{r\_\text{extreme}} = ((G+\varepsilon)/(2(G-\varepsilon)))$, for which we can write

$$I_{H\_\max}^k = \frac{1}{4F}\frac{(G+\varepsilon)^2}{(G-\varepsilon)}.$$

Thus, the exact value of X_r is either bounded by $X_{r\_\min} \leq X_r \leq X_{r\_\text{extreme}}$ or $X_{r\_\text{extreme}} \leq X_r \leq X_{r\_\max}$. Therefore, in the two cases, I_H^k is bounded by

$$\frac{G\varepsilon}{(G-\varepsilon)F} \leq I_H^k(X_r) \leq \frac{1}{4F}\frac{(G+\varepsilon)^2}{(G-\varepsilon)}.$$

We define the relative measure of the tightness between the upper and lower bound of I_H^k as

$$\Delta(G,\varepsilon) = \frac{I_{H\_\max}^k - I_{H\_\min}^k}{I_{H\_\min}^k} = \frac{(G-\varepsilon)^2}{4G\varepsilon}.$$

We can see clearly that $\lim_{\varepsilon\to G}\Delta(G,\varepsilon) = 0$, which makes the two bounds converge asymptotically to the same value

$$I_H^k = \frac{G\varepsilon}{(G-\varepsilon)F}.$$

Using this result in (39), we obtain (42). ■

References

[1] J. G. Zhang, "Novel optical fiber code-division multiple-access networks supporting real-time multichannel variable-bit-rate (VBR) video distributions," *IEEE Trans. Broadcasting*, vol. 43, pp. 339–349, Sep. 1997.

[2] ——, "Design of a special family of optical CDMA address codes for fully asynchronous data communications," *IEEE Trans. Commun.*, vol. 47, pp. 967–973, Jul. 1999.

[3] S. Maric, O. Moreno, and C. J. Corrada, "Multimedia transmission in fiber optical LAN's using optical CDMA," *IEEE J. Lightwave Technol.*, vol. 14, pp. 2149–2153, Oct. 1996.

[4] G.-C. Yang, "Variable-weight optical orthogonal codes for CDMA networks with multiple performance requirements," *IEEE Trans. Commun.*, vol. 44, pp. 47–55, Jan. 1996.

[5] E. Inaty, L. A. Rusch, and P. Fortier, "Multirate optical fast frequency hopping CDMA system using power control," *IEEE J. Lightwave Technol.*, vol. 20, pp. 166–177, Feb. 2002.

[6] H. Fathallah, L. A. Rusch, and S. Larochelle, "Passive optical fast frequency hop CDMA communication system," *IEEE J. Lightwave Technol.*, vol. 17, pp. 397–405, Mar. 1999.

[7] E. Inaty, H. M. H. Shalaby, and P. Fortier, "A new transmitter-receiver architecture for noncoherent multirate OFFH-CDMA system with fixed optimal detection threshold," *IEEE J. Lightwave Technol.*, vol. 20, pp. 1885–1894, Nov. 2002.

[8] E. Inaty, P. Fortier, and L. A. Rusch, "SIR performance evaluation of a multirate OFFH-CDMA system," *IEEE Commun. Lett.*, vol. 5, pp. 224–226, Apr. 2001.
[9] L. D. Wronski, R. Hossain, and A. Albicki, "Extended hyperbolic congruential frequency hop code: Generation and bounds for cross- and auto-ambiguity function," *IEEE Trans. Commun.*, vol. 44, pp. 301–305, Apr. 1996.
[10] L. Bin, "One-coincidence sequences with specified distance between adjacent symbols for frequency-hopping multiple access," *IEEE Trans. Commun.*, vol. 45, pp. 408–410, Apr. 1997.

Elie Inaty (S'99–M'02) was born in El-Koura, North Lebanon, on June 23, 1975. He received the B.S. and M.S. degrees in electrical engineering from the University of Balamand, El-Koura, North Lebanon, in 1996 and 1998, respectively, and the Ph.D. degree from Université Laval, Quebec, QC, Canada, in 2001.

He is currently an Assistant Professor at the University of Balamand. His research interests include CDMA and WDM fiber optic communications, network-control and resource-management issues in optical communication networks, and radio multiple-access techniques.

Hossam M. H. Shalaby (S'83–M'91–SM'99) was born in Giza, Egypt, in 1961. He received the B.S. and M.S. degrees from the University of Alexandria, Alexandria, Egypt, in 1983 and 1986, respectively, and the Ph.D. degree from the University of Maryland, College Park, in 1991, all in electrical engineering.

In 1991, he joined the Department of Electrical Engineering, University of Alexandria, as an Assistant Professor. He was promoted to the position of Associate Professor in 1996, and then to Professor in 2001 (current position). Since December 2000, he has been an Adjunct Professor with the Department of Electrical and Information Engineering, Faculty of Sciences and Engineering, Laval University, Quebec, QC, Canada. From March to April 1996, he was a Visiting Professor at the Electrical Engineering Department, Beirut Arab University, Beirut, Lebanon. From September 1996 to January 1998, he was an Associate Professor with the Electrical and Computer Engineering Department, International Islamic University Malaysia, Kuala Lumpur, Malaysia, and from February 1998 to December 1998, he was with the School of Electrical and Electronic Engineering, Nanyang Technological University, Singapore, where he was a Senior Lecturer, and from January 1999 to February 2001, an Associate Professor. His research interests include optical communications, optical CDMA, spread-spectrum communications, and information theory.

Dr. Shalaby received the SRC fellowship from 1987 to 1991 from the Systems Research Center, MD, the Shoman Prize for Young Arab Researchers in 2002 from the Abdul Hameed Shoman Foundation, Amman, Jordan, the State Award twice in 1995 and 2001 from the Academy of Scientific Research and Technology, Egypt, the University Award in 1996 from the University of Alexandria, and the Soliman Abd-El-Hay Award in 1995 from the Academy of Scientific Research and Technology, Egypt. He has served as a Student Branch Counselor for Alexandria University, IEEE Alexandria and North Delta Subsection, since 2002, and served as a Chairman of the Student Activities Committee of the IEEE Alexandria Subsection from 1995 to 1996. He has also served as a technical referee for *Proceedings of the Institution of Electrical Engineers*, the IEEE TRANSACTIONS ON COMMUNICATIONS, the IEEE TRANSACTIONS ON INFORMATION THEORY, the IEEE JOURNAL ON SELECTED AREAS IN COMMUNICATIONS, and the IEEE/OSA JOURNAL OF LIGHTWAVE TECHNOLOGY. He is listed in the 14th edition of *Marquis Who's Who in the World*, 1997.

Paul Fortier (S'79–M'82–SM'00) received the B.Sc. and M.Sc. degrees in electrical engineering from Laval University, Québec, QC, Canada, in 1982 and 1984, respectively, and the M.S. degree in statistics and the Ph.D. degree in electrical engineering from Stanford University, Stanford, CA, in 1987 and 1989, respectively.

Since 1989, he has been with the Department of Electrical and Computer Engineering at Laval University, where he is currently a full Professor. From 1991 to 1997, he was Program Director for the B.Sc. degree in Computer Engineering, and from 1997 to 2003, he was Chairman of the Department of Electrical and Computer Engineering. Since 2003, he has been Associate Dean for development and Research at the Faculty of Science and Engineering. He has done consulting work for several companies and government agencies in Canada. His research interests include digital signal processing for communications, and the study of complexity and performance trade-offs in hardware implementations, with applications in wireless and optical communications. He has been involved in the organization of national and international conferences and workshops in these fields.

Dr. Fortier is a Fellow of the Engineering Institute of Canada.